

Chapter 22

Microslip Joint Damping Prediction Using Thin-Layer Elements

Christian Ehrlich, André Schmidt, and Lothar Gaul

Abstract In this work, an efficient FE-modeling technique for assembled metallic structures is presented. Linear thin-layer elements containing damping and stiffness parameters are placed on the interfaces of bolted joints. The interface parameters are identified experimentally on an isolated lap joint and then used as an input for the FE-simulation. Since the presented modeling technique is linear, it delivers acceptable results only for small relative displacements in the joint interface, i.e. microslip. Therefore investigations on the transition from micro- to macroslip are conducted. A promising approach to detect macroslip is based on the significant increase of higher harmonic frequency generation. The application of this criterion results in a linear relation between the normal force and the maximum tolerable tangential force.

Keywords Joints • Damping • Thin-layer elements • Nonlinear effects • Finite element method

22.1 Introduction

Eigenfrequencies and mode shapes, even those of complex structures, can be predicted accurately with the Finite Element Method. However, correct decisions in the design phase as to whether the vibrational and acoustic properties of a certain design are satisfactory, cannot be made without knowledge of the amplitude of the vibration. Estimating modal amplitudes is only possible with an accurate damping model. Since there is no recognized, simple and accurate method for predicting the dissipative properties of complex structures, the industry either ignores damping or uses a rule of thumb. This paper presents an approach for the prediction of damping of a structure in the design phase. This method is only applicable if no nonlinearities introduced by macroslip are present. Therefore a method to distinguish between micro- and macroslip based on the nonlinearity is developed.

In a structure assembled solely with bolted joints there are two major contributors to energy dissipation (ignoring acoustic radiation and gas pumping): material damping and joint damping. Material damping is caused by inner friction within a material [8]. Therefore its effect appears throughout the entire structure and influences all modes equally. Joint damping is the paramount influence factor to modal damping of an assembled structure. Generally it is about 10–100 times higher than material damping and only occurs locally at the interface of two members. Therefore it has varying influence on different modes, depending on the participation of the interface in the particular mode.

Experimental investigations have shown that material damping and joint damping are both weakly dependent on frequency [4]. Therefore the model of constant hysteretic damping, which assumes the dissipated energy per cycle to be independent of the frequency, is applied.

In order to depict the local influence of the joint damping, thin-layer elements (TLEs) are placed on all interfaces of the assembled structure [3]. Those elements contain the stiffness and the loss factor of the joint and preserve the localization of the interface damping. Material damping is modeled using a global loss factor.

The material properties for the TLEs are determined experimentally on an isolated lap joint.

C. Ehrlich (✉) • A. Schmidt • L. Gaul

Institute of Applied and Experimental Mechanics, University of Stuttgart, Pfaffenwaldring 9, 70550 Stuttgart, Germany
e-mail: ehrllich@iam.uni-stuttgart.de

Fig. 22.1 Experimental setup for joint parameter extraction

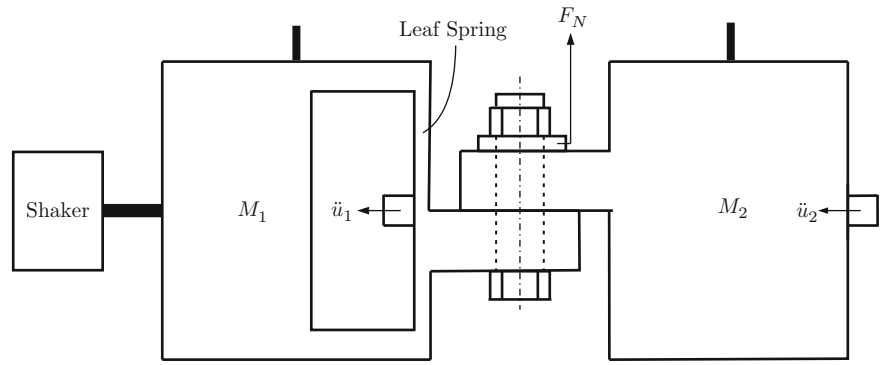
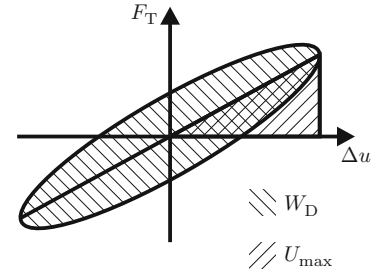


Fig. 22.2 Schematic hysteresis curve



22.2 Experimental Joint Parameter Extraction

In order to determine the parameters needed to predict the damping behavior of a complex structure, measurements on an isolated, representative joint are conducted. The experimental setup is depicted in Fig. 22.1. It consists of two masses M_1 and M_2 , each supported by thin wires at their respective center of gravity and connected with a steel lap joint. It is important to assure that the joint in the experiment reflects the joint in the assembled structure as accurately as possible. Therefore key characteristics like the materials, surface finish, and normal pressure have to be equal. M_1 features a leaf spring which improves the system response drastically. The structure is excited with a shaker and when the system is in steady state, the accelerations \ddot{u}_1 and \ddot{u}_2 are recorded with accelerometers. Additionally, the normal force in the joint F_N is monitored with a force measuring ring.

The transmitted force F_T can be calculated as product of \ddot{u}_2 and M_2 . The relative displacement Δu in the joint can be computed as the difference of the displacements u_1 and u_2 of the Masses M_1 and M_2 . The displacements are obtained by integrating \ddot{u}_1 and \ddot{u}_2 twice. Plotting the transmitted force over the relative displacement yields the hysteresis curve. The stiffness is given as the slope of the hysteresis curve. The loss factor η is defined as the dissipated energy per cycle W_D divided by 2π times the maximum stored energy U_{\max}

$$\eta = \frac{W_D}{2\pi U_{\max}}. \quad (22.1)$$

The graphical representation of W_D and U_{\max} is depicted in Fig. 22.2.

Once the joint parameters are extracted, they serve as an input to the FE simulation. The influence of different normal and tangential forces on the joint parameters and the applicability of the modeling technique will be discussed Sect. 22.4. Previous work shows no significant influence of the frequency on loss factor and stiffness [1].

22.3 FE Simulation

Due to the weak dependency of both, material damping and joint damping, on frequency, the model of constant hysteretic damping is applied [7]. This approach is only valid in the frequency domain since it is not causal in the time domain [5]. Previous work shows good correlation with experimentally determined parameters [1].

Starting point for the simulation is the equation of motion for a free undamped system

$$\underline{M} \ddot{\underline{u}} + \underline{K} \underline{u} = \underline{0}, \quad (22.2)$$

where \underline{M} is the mass matrix, \underline{K} is the real-valued stiffness matrix and \underline{u} is the displacement vector.

Using the model of constant hysteretic damping, the undamped model can be modified to include damping. For that purpose, the frequency independent damping will be incorporated into the stiffness matrix by adding the complex-valued product of the dissipation multipliers (α_i for the material and β_i for the joints) and the associated elements stiffness matrices $\underline{K}^{(\text{Material})}$ and $\underline{K}^{(\text{Joint})}$

$$\underline{K}^* = \underline{K} + j \sum_{i=1}^n \alpha_i \underline{K}_i^{(\text{Material})} + j \sum_{i=1}^m \beta_i \underline{K}_i^{(\text{Joint})}. \quad (22.3)$$

Complex modal analysis can be performed on the modified equation of motion, yielding complex eigenvectors and eigenvalues. From the complex eigenvalues, modal damping factors can be extracted, which are the central goal of this analysis.

Before this is possible, the elasticity matrix of the TLEs has to be determined. For that purpose, a TLE under shear deformation is considered. For a linear material the shear stress τ is given by

$$\tau = G\gamma \approx G \frac{\Delta u}{d}, \quad (22.4)$$

where G is the shear modulus, γ is the shear angle, Δu the relative tangential displacement and d the thickness of the TLE. Furthermore, the shear stress can be approximated by the ratio of the tangential force F_T and the area of the contact patch A

$$\tau = \frac{F_T}{A}. \quad (22.5)$$

Combining Eqs. (22.4) and (22.5) yields

$$F_T = \frac{GA}{d} u = cu, \quad (22.6)$$

where c is the experimentally extracted stiffness. Measuring c and A , the shear modulus for the TLEs can be calculated as

$$G = \frac{cd}{A}. \quad (22.7)$$

It is important to note that G depends on d , which means it must be adapted when the thickness of the TLEs is modified.

At this point, one must consider the orthotropic characteristic of bolted joints with decisively different behavior in normal and tangential direction. The tangential parameters have major influence on the overall behavior of the structure, whereas the normal parameters have little influence [10]. This leads to two conclusions. First, the TLEs should be modeled with orthotropic behavior. Second, experimental determination of the tangential parameters is sufficient. Normal parameters can be estimated. Orthotropic behavior leads to the following constitutive equation for the TLEs

$$\begin{bmatrix} \sigma_{xx} \\ \sigma_{yy} \\ \sigma_{zz} \\ \sigma_{xy} \\ \sigma_{yz} \\ \sigma_{zx} \end{bmatrix} = \begin{bmatrix} E_{11} & E_{12} & E_{13} & 0 & 0 & 0 \\ & E_{22} & E_{23} & 0 & 0 & 0 \\ & & E_{33} & 0 & 0 & 0 \\ & & & E_{44} & 0 & 0 \\ & & & & E_{55} & 0 \\ & & & & & E_{66} \end{bmatrix} \begin{bmatrix} \epsilon_{xx} \\ \epsilon_{yy} \\ \epsilon_{zz} \\ \epsilon_{xy} \\ \epsilon_{yz} \\ \epsilon_{zx} \end{bmatrix}. \quad (22.8)$$

Since there is no transversal contraction in the interface, the off-diagonal terms are zeros. Accordingly E_{11} , E_{22} , and E_{44} vanish because the interface has no stiffness parallel to the interface or for in-plane shearing. E_{33} represents the normal stiffness and $E_{55} = E_{66} = G$ define the tangential stiffness.

The validity of this modeling approach is demonstrated in [1]. There, numerical and experimental modal analysis are performed for a simple U-shaped structure. For the simulation, joint parameters are extracted from a generic experiment.

The first 10 modes of the structure are analyzed. For 8 of those modes, the predicted damping is within 25 % of the experimental value. The other two modes differ by 58 and 89 %. Considering the sensitivity of damping and the simplicity of the modeling approach, these are good results.

22.4 Differentiation Between Micro- and Macroslip

The presented modeling technique is linear which requires careful definition of the limits of its applicability.

A very important distinction in this context is between microslip and macroslip. Microslip occurs under high normal and/or low tangential forces. Small areas of the contact area slip, while a large part of the contact is still sticking. If the normal forces are decreased and/or the tangential forces increased, the components start to globally move relative to each other. This is called macroslip. While macroslip always introduces significant nonlinearity, in its absence, joint damping can still be linearized with acceptable accuracy [2]. Therefore a reliable parameter to indicate the presence of macroslip is needed.

In order to investigate the transition from micro- to macroslip experiments with the basic setup of Fig. 22.1 are conducted. For different normal force levels, the tangential load is increased until macroslip is prevalent.

Examining the hysteresis curves for different tangential loads gives a good first insight into the process. Instead of plotting F_T over Δu , \ddot{u}_2 over \ddot{u}_1 is used. Those curves show the same basic behavior but the influence of higher harmonic frequencies, e.g. non-linearities, is more apparent.

Figure 22.3 illustrates the transition from micro- to macroslip. Data for measurements at a normal force of 1,500 N and increasing tangential forces of 80, 110, and 250 N, are depicted. In the case of pure microslip, as in Fig. 22.3a, the hysteresis is typically very thin, indicating a low loss factor. Only rotating and rescaling reveals the shape which is close to an ellipse. A linear system with constant hysteretic damping shows a perfectly elliptic hysteresis loop. In the macroslip regime (Fig. 22.3c), the hysteresis curve opens significantly, showing the increase in dissipated energy. Also, the shape changes to a lancet with clearly visible sliding at the tips.

In the case of harmonic excitation, it is obvious, that the transition from micro- to macroslip must be a gradual process. As the excitation amplitude is increased, larger and larger portions of the transmitted force will exceed the maximum transferable force, therefore resulting in more and more macroslip. Therefore finding a crisp barrier between the two regimes is unlikely.

Even though evaluating the shape of the hysteresis curve provides very direct information about the occurrence of slip, it does not serve well as a sole decision criterion. It is slow, subjective, and unquantifiable. It is also not precise because a significant amount of macroslip and nonlinearity have to be present for the hysteresis curve to be visibly deformed. Other parameters to indicate the presence of macroslip are based on the progression of the loss factor and the dissipated energy [9]. However, they lack the precision needed in this case.

Yet, the observation of the hysteresis curve can be the basis to a better decision strategy. First, one has to examine the curves more closely, in order to be able to detect the first occurrence of macroslip more accurately. For that purpose one can rotate and rescale them. Figure 22.4 shows the curves of Fig. 22.3a, b. While Fig. 22.4a shows good correlation to an ellipse, Fig. 22.4b clearly deviates from that shape. Now that more precise information about the transition is available, it can be linked to the original cause for the deformation: higher harmonic frequency components. As a nonlinearity parameter, the ratio of the third harmonic amplitude A_3 and the base amplitude A_1 of the acceleration is defined

$$\kappa = \frac{A_3}{A_1}. \quad (22.9)$$

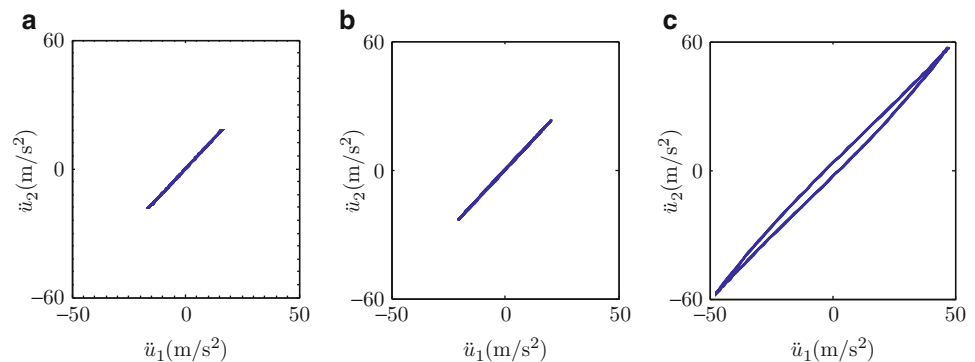


Fig. 22.3 Typical hysteresis curves for microslip (a), transition (b) and macroslip (c)

Fig. 22.4 Rotated and scaled hysteresis curves without (a) and with (b) significant deformation due to macroslip

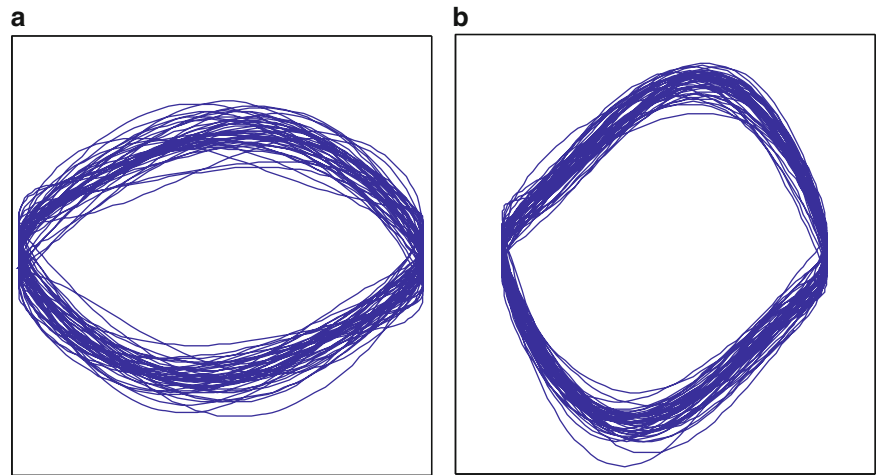
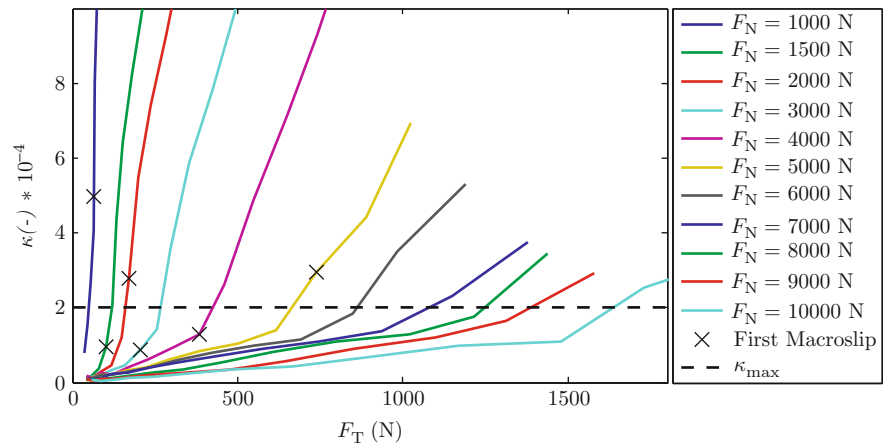


Fig. 22.5 Nonlinearity parameter for different normal and tangential forces



Since the third harmonic amplitude is the largest among the higher harmonic frequency components, it is chosen as the indicator for nonlinearity. For normal forces from 1,000 to 5,000 N, the appearance of macroslip can always be linked to a nonlinearity $0.9 \times 10^{-4} < \kappa < 5.0 \times 10^{-4}$. For higher normal forces, the hysteresis curve becomes so narrow that rescaling does not work reliably. Therefore the transition cannot be monitored as accurately. Still, a transition within the specified nonlinearity range is expected. Figure 22.5 shows the nonlinearity parameter for different normal forces and tangential forces. Additionally, the first measurement with clearly visible macroslip is marked.

Defining a barrier between micro- and macroslip is now a matter of finding a reasonable κ value. In this case $\kappa_{\max} = 2 \times 10^{-4}$ is chosen. Even though this allows for macroslip in some cases, the nonlinearity overall is still very low. Obviously there is significant uncertainty in defining a value for κ_{\max} . This stems from the gradual nature of the transition and measurement inaccuracy. The uncertainty can be dealt with mathematically by applying Fuzzy arithmetic [6], which is not within the scope of this paper.

Applying κ_{\max} to the presented measurements leads to a set of maximum tolerable tangential forces as a function of the normal force. As can be seen in Fig. 22.6, a straight line can be fitted well to the data. Thus, the limit of applicability of the presented modeling technique can be expressed by a single parameter. For the steel joint under investigation in this work, a slope of $\mu = 0.15$ is determined. Choosing $\kappa_{\max} = 0.9 \times 10^{-4}$, the lowest nonlinearity for which macroslip can be observed, results in $\mu = 0.09$.

Figure 22.7 shows the loss factor and the dissipated energy for different excitation forces and a constant normal force of 1,500 N. Additionally the maximum tolerable tangential force is marked with “x”. It can be seen, that both parameters stay almost constant below the defined transition. Therefore the uncertainty of the input parameters is restricted.

Having extracted μ , one can now check the application at hand. If the applied tangential load is lower than the tolerable force considering the applied normal force, macroslip will be avoided and the presented modeling approach is applicable.

Fig. 22.6 Maximum tolerable tangential force as function of the normal force

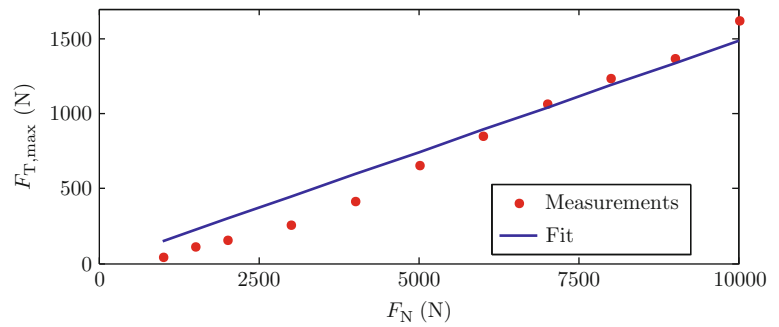
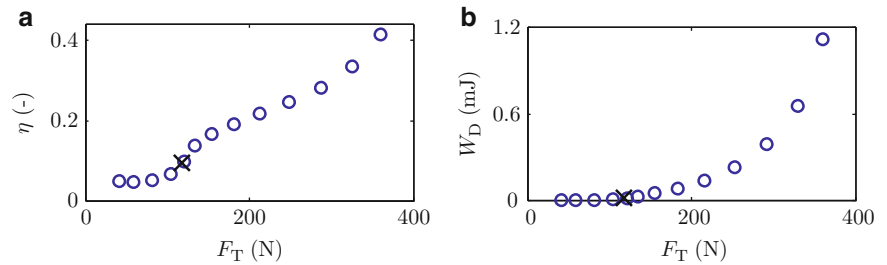


Fig. 22.7 (a) Loss factor and (b) dissipated energy for different excitation forces



22.5 Conclusion

A simple modeling technique to predict damping characteristics of assembled structures is presented. Thin-layer elements are employed to preserve the localization of joint damping. The parameters for the simulation are acquired experimentally on an isolated lap joint.

Since the presented method is linear, it only delivers acceptable results when no macroslip occurs. Experimental investigation on the transition from micro- to macroslip show that higher harmonic amplitudes serve well as an indicator for the presence of macroslip. A nonlinearity parameter based on the third harmonic amplitude is used to define the limit of applicability of the presented modeling approach. This leads to a linear relation between the maximum tolerable tangential force and the normal force. A given assembled structure may be simulated with the presented technique if the applied tangential load is less than the maximum tolerable tangential force, given the normal force.

References

1. Bograd S, Schmidt A, Gaul L (2008) Joint damping prediction by thin layer elements. In: Proceedings of IMAC XXVI: a conference and exposition on structural dynamics, Orlando, 2008
2. Bograd S, Reuss P, Schmidt A, Gaul L, Mayer M (2011) Modeling the dynamics of mechanical joints. *Mech Syst Signal Process* 25(8): 2801–2826
3. Desai CS, Zaman MM, Lightner JG, Siriwardane HJ (1984) Thin-layer element for interfaces and joints. *Int J Numer Anal Method Geomech* 8(1):19–43. ISSN 1096-9853. doi:10.1002/nag.1610080103. <http://dx.doi.org/10.1002/nag.1610080103>
4. Ewins DJ (2000) *Modal testing: theory, practice and application*, vol 2. Research Studies Press, Baldock
5. Gaul L, Klein P, Kemple S (1991) Damping description involving fractional operators. *Mech Syst Signal Process* 5(2):81–88
6. Hanss M (2002) The transformation method for the simulation and analysis of systems with uncertain parameters. *Fuzzy Set Syst* 130(3): 277–289
7. Lakes RS (1999) *Viscoelastic solids*, vol 9. CRC Press, Boca Raton
8. Lazan BJ (1968) *Damping of materials and members in structural mechanics*, vol 214. Pergamon Press, Oxford
9. Lenz J (1997) *Strukturdynamik unter dem Einfluss von Mikro- und Makroschlupf in Fugestellen*. Ph.D. thesis, Inst. A für Mechanik
10. VDI Richtlinie 3830: Damping of Materials and Members, 2005